VOL. 17, NO. 8, APRIL 2022 ISSN 1819-6608
ARPN Journal of Engineering and Applied Sciences

www.arpnjournals.com

YAW MOVEMENT IDENTIFICATION OF AN UNMANNED AERIAL VEHICLE USING A FREQUENCY DOMAIN METHOD

Faiber Robayo Betancourt[1], Fredy H. Martínez S[2] and Daniel Suescún-Díaz[3]
[1]Departamento de Ingeniería Electrónica, Facultad de Ingeniería, Universidad Surcolombiana, Neiva, Huila, Colombia
[2]Facultad Tecnológica, Universidad Distrital Francisco José de Caldas, Bogotá D.C., Colombia
[3]Departamento de Ciencias Naturales, Avenida Pastrana, Universidad Surcolombiana, Neiva, Huila, Colombia
E-mail: faiber.robayo@usco.edu.co

ABSTRACT

In this work, a frequency domain method based on the Transfer Function Analyzer (TFA) technique to identify the yaw movement of an unmanned aerial vehicle (UAV) helicopter was presented. This study's contribution was to use a variable sample time instead of the traditional fixed sample time. The Transfer Function Analyzer identification was compared with an identification method using CIFER (Comprehensive Identification from Frequency Responses), a commercially available tool designed for aircraft identification. The two results were quite close for the two experiments.

Keywords: frequency domain identification, unmanned aerial vehicle, CIFER, transfer function analyzer, chirp signal.

1. INTRODUCTION

System identification is a general term used to describe mathematical tools and algorithms that build dynamical models from measured data. Frequency domain experimental data are common in many applications, especially in application areas where experimental data of a process with unknown dynamics can be taken relatively cheaply. The excitation of the process with periodic signals (e.g., sinusoids) is an attractive way of extracting accurate information of the process dynamics from experiments. Due to the commercial availability of frequency analyzers that can handle large amounts of data by special-purpose hardware, the experimental determination of frequency response of dynamic systems has increased interest in application areas as the modeling of mechanical servo systems [1-4].

Identification based on frequency domain data has some advantages when compared to the "classical" time-domain approach. An overview of the advantages of identification based on frequency response data compared to time-domain approach is given in [5].

The formulation of an identification criterion in the frequency domain can be useful, especially in those situations where the application of the model dictates a performance evaluation in terms of frequency domain properties. This latter situation often occurs when the identified models are used as a basis for model-based control design. On the other hand, it should be worried that any frequency domain data is obtained by some data handling/processing mechanism that starts with time-domain data. This situation is a reason not to overestimate the difference between time-domain and frequency-domain identification; see, e.g., [1].

The conventional way of formulating an identification problem in the frequency domain is by assuming the availability of the exact frequency response of the (unknown) linear system, disturbed by some additive noise. Many identification methods exist for this situation, mostly dealing with the least-squares criteria [6], [7]. Recently subspace algorithms also have been analyzed for frequency domain identification [8]. Many more references and techniques can be found in [9].

A related approach to the problem based on the discrete Fourier transforms of input and output data in [1] shows a close similitude of results with the standard time-domain approach.

Frequency response analysis (FRA) is a very well established system identification method [9]. The technique has remained over other techniques simply because it is so simple, flexible, and robust. For example, the use of frequency response methods to measure the response of systems while under closed-loop control has been established for many years. Whereas closed-loop estimation using other methods of identification takes much longer to catch up and even require expert knowledge to apply them. The same is true of nonlinear systems and systems where the input or output signals are noise corrupted. FRA methods deal with such issues routinely while alternative methods need specialized experience.

The present study aimed to use a frequency domain method based on the Transfer Function Analyzer technique applied for the identification of the yaw movement of a UAV helicopter (rotation in a plane parallel to the surface of the Earth). Yaw movement is achieved by making the two rotors of the helicopter spin at different angular rates, which will result in a torque on the body of the helicopter. Two DC motors drive the rotors. In a recent study, a PID controller was applied for the yaw movement of the coaxial helicopter in [10].

2. MATERIALS AND METHODS

2.1 Yaw Movement in an Unmanned Aerial Vehicle

The information used for this work was taken from the thesis [11] in which they used an identification method provided by CIFER, a commercially available tool designed for aircraft identification. We focused just on the identification part to compare those results with our identification method using TFA.

The application presented in this work is a UAV platform based on a commercially available coaxial helicopter shown in Figure-1.

Figure-1. Coaxial helicopter.

2.2 Frequency Response Analysis

Frequency response analysis is the technique where a sinusoidal test signal is used to measure points on the frequency response of a transfer function or impedance function. Figure-2 shows the scheme in which a sine wave $u(t)$ is applied to a system with transfer function $G(s)$. After transients due to initial conditions have declined, the output $y(t)$ will be a sine wave but with a different magnitude b and phase shift φ.

Figure-2. Linear transfer function with sinusoidal input.

Figure-3 depicts the input and output signals, where as:

$$u(t) = a\sin(\omega t) \text{ and } y(t) = b\sin(\omega t + \varphi)\ ; \omega = 2\pi f = \frac{2\pi}{T}$$

with $f = \frac{1}{T}$, the frequency in Hz.

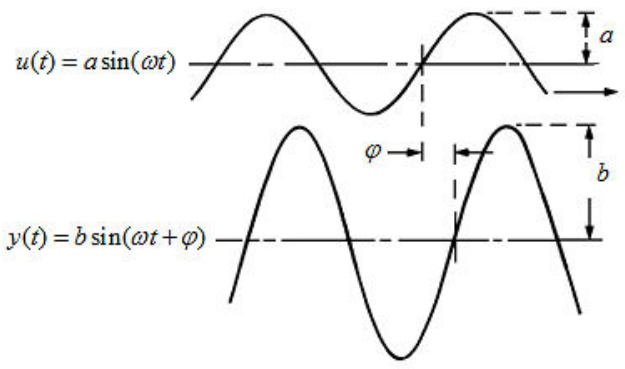

Figure-3. Sinusoidal input (up) and sinusoidal response (down).

The magnitude and phase of the output $y(t)$ are related to the transfer function $G(s)$ at the frequency (ω *rad/s*) of the input sinusoid as:

$\frac{b}{a} = |G(i\omega)|$ is the gain at ω

$\varphi = \angle |G(i\omega)|$ is the phase at ω

For several measurements of the gain and phase at various frequencies, a diagram of the system frequency response can be plotted either as a Nyquist diagram in the complex plane or a Bode diagram as shown in Figure-4.

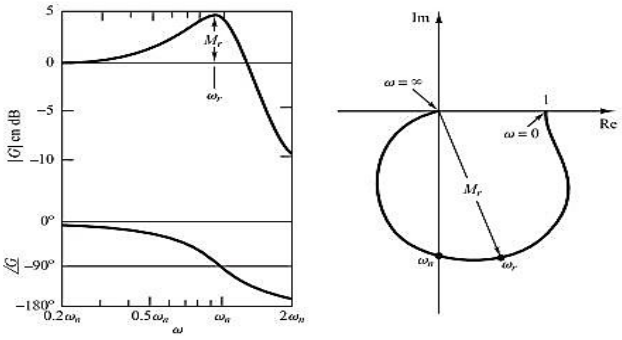

Figure-4. Frequency response diagrams, Nyquist (right) and Bode (left).

2.3 General TFA Approach (One Sinusoidal Input)

The relative phase and magnitude of the input and the output waveforms can be directly measured from an oscilloscope trace (Figure-3). However, this measurement has reduced accuracy, and more sophisticated methods are required to remove specific errors that occur due to noise and non-linearity. Signal corruption is due to external noise which infects the output measurements; thus the output $y(t)$ is:

$$y(t) = b\sin(\omega t + \varphi) + n(t) \quad (1)$$

Where $n(t)$ represents the noise.

Both the problems of non-linear distortion and noise corruption are overcome in the measurement scheme of Figure-5, in which the measured output $y(t)$ is first multiplied by sine and cosine respectively and then integrated.

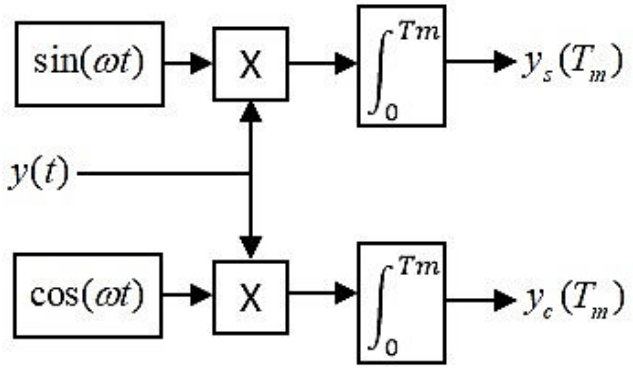

Figure-5. TFA implementation.

In Figure-5, the output $y(t)$ is first multiplied by a sine and cosine of the test frequency ω then the result of the multiplications are integrated over T_m seconds. Integrating for one period, we obtain:

$$y_s(T_m) = \int_0^{T_m} y(t)\sin(\omega t)dt \quad (2)$$

$$y_s(T_m) = \int_0^{T_m} b\sin(\omega t+\varphi)\sin(\omega t)dt + \int_0^{T_m} n(t)\sin(\omega t)dt \quad (3)$$

We apply a product to sum formula for the quantity in the first integral:

$$\sin(\omega t+\varphi)\sin(\omega t) = \frac{1}{2}[\cos(\varphi)-\cos(2\omega t+\varphi)] \quad (4)$$

We thus obtain:

$$y_s(T_m) = \int_0^{T_m}\frac{b}{2}\cos\varphi - \int_0^{T_m}\frac{b}{2}\cos(2\omega t+\varphi)dt + \int_0^{T_m} n(t)\sin(\omega t)dt \quad (5)$$

$$y_s(T_m) = \frac{b}{2}T_m\cos\varphi - \frac{b}{2}\int_0^{T_m}\cos(2\omega t+\varphi)dt + \int_0^{T_m} n(t)\sin(\omega t)dt \quad (6)$$

Analogously,

$$y_c(T_m) = \int_0^{T_m} y(t)\cos(\omega t)dt \quad (7)$$

$$y_c(T_m) = \int_0^{T_m} b\sin(\omega t+\varphi)\cos(\omega t)dt + \int_0^{T_m} n(t)\cos(\omega t)dt \quad (8)$$

We apply a product to sum formula for the quantity in the first integral:

$$\sin(\omega t+\varphi)\cos(\omega t) = \frac{1}{2}[\sin(\varphi)+\sin(2\omega t+\varphi)] \quad (9)$$

and thus obtain:

$$y_c(T_m) = \int_0^{T_m}\frac{b}{2}\sin\varphi + \int_0^{T_m}\frac{b}{2}\sin(2\omega t+\varphi)dt + \int_0^{T_m} n(t)\cos(\omega t)dt \quad (10)$$

$$y_c(T_m) = \frac{b}{2}T_m\sin\varphi + \frac{b}{2}\int_0^{T_m}\sin(2\omega t+\varphi)dt + \int_0^{T_m} n(t)\cos(\omega t)dt \quad (11)$$

As the averaging time increases, the contribution of all unwanted frequency components in $y_s(T_m)$ and $y_c(T_m)$ go to zero. In practice, the averaging is conducted over a finite time interval T_m, and it is necessary, that T_m be made an integer multiple of the test frequency period. If one integrates on a multiple of half the period for a particular frequency, one can observe that the second term in equations (6) and (11) will be zero. If we consider the integration time to be long enough, the noise will be filtered out (i.e., zero average). Thus, we can write:

$$y_s(T_m) \approx \frac{b}{2}T_m\cos\varphi \quad (12)$$

$$y_c(T_m) \approx \frac{b}{2}T_m\sin\varphi \quad (13)$$

From equations (12) and (13) we deduce that:

$$b = \frac{2}{T_m}\sqrt{y_s^{\,2}(T_m)+y_c^{\,2}(T_m)} \quad (14)$$

$$\varphi = a\tan\frac{y_c(T_m)}{y_s(T_m)} \quad (15)$$

Plotting the b and φ values for a range of frequencies we can obtain a Bode diagram for the identified system.

2.4 TFA Concept with a Chirp Signal

As explained in section 2.2, several sinusoidal test signals at different frequencies are used to measure points on the frequency response of a transfer function. Now the approach is to obtain the response for the whole range of frequencies by sending just one identification signal. The frequency of this sinusoidal test signal should vary from a minimum frequency (f_0) till a maximum frequency (f_1) in a specific time T. This signal is commonly named "Chirp signal". The sampling period of the signal will also vary according to frequency, to maintain the same sampling resolution for all frequencies. Then, we will use a fixed number of data points (N_s) to sample one period independently of the frequency. An example of the mentioned chirp signal is showed in Figure-6.

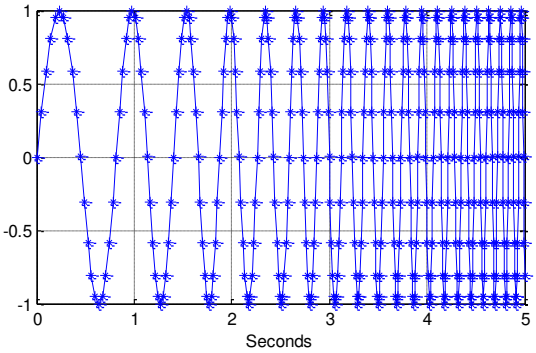

Figure-6. Chirp signal from 1 to 10 Hz in 5 seconds, 20 points per period.

In Figure-6, it is possible observe that each period is sampled with exactly 20 points. To processing the data, we will divide the chirp signal into fragments, which can be considered to have the same frequency. Each of these fragments will be used to obtain one point for gain and one point for the phase in the Bode diagram of the system. The scheme of the TFA discrete implementation is depicted in Figure-7.

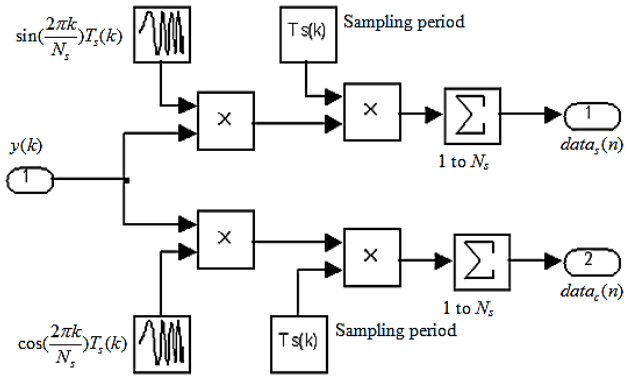

Figure-7. Scheme of the TFA discrete implementation.

To the chirp generation se should consider that $\sin 2\pi \cdot f \cdot t = \sin 2\pi \cdot f(t) \cdot kT_s(t)$. We should choose al every moment t, a variable time step $T_s(t)$ such that 1 period contains N_s samples; so we must select $T_s(t)$ such that $f(t) \cdot T_s(t) = \frac{1}{N_s}$.

The N_s samples are then given by $\sin(\frac{2\pi k}{N_s})$, with $k = 0,1...N_s - 1$.

Consider that we choose to split the chirp signal into intervals of one period. If we were to numerically apply equations (6) and (11) on the nth interval, we would obtain:

$$data_s(n) = \sum_{k=N_s(n-1)}^{N_s n-1} y(k)\sin(\frac{2\pi k}{N_s})T_s(k) \quad (16)$$

$$data_c(n) = \sum_{k=N_s(n-1)}^{N_s n-1} y(k)\cos(\frac{2\pi k}{N_s})T_s(k) \quad (17)$$

$T_s(k)$ represents the sampling time at the k^{th} sample in the data vector. $T_s(k)$ should respect the next relation:

$$T_s(k) = \frac{1}{N_s f(k)} \quad (18)$$

Where $f(k)$ represents the frequency at the k^{th} sample. The linear instantaneous frequency at the time t, can be found as:

$$f(t) = f_0 + \frac{(f_1 - f_0)}{T}t \quad (19)$$

Considering we obtain one point in a Bode plot for each period on which we integrate, it makes sense to increase frequency exponentially with time, to get the same resolution (points per decade) for all frequency intervals in the plot. Therefore, frequency is calculated as:

$$\log f(t) = \log f_0 + \frac{(\log f_1 - \log f_0)}{T}t \quad (20)$$

$$\log \frac{f(t)}{f_0} = \log \frac{f_1}{f_0}\frac{t}{T} \quad (21)$$

$$\log \frac{f(t)}{f_0} = \log(\frac{f_1}{f_0})^{\frac{t}{T}} \quad (22)$$

$$f(t) = f_0(\frac{f_1}{f_0})^{\frac{t}{T}} \quad (23)$$

3. RESULTS AND DISCUSSIONS

3.1 Hypothetical Model of Yaw Rotation

Let us regard the mechanical equation for the torque on the shaft of a motor (24) in the case of the helicopter:

$$\tau = J\frac{d\omega}{dt} + B\omega \quad (24)$$

Where τ the torque is generated by the DC engine on its shaft, J is the moment of inertia of the rotating mass, ω is the angular rate of the rotor and B is the viscous friction coefficient.

The parameter J represents the moment of inertia of the rotors. The parameter B refers to the opposing force from the air, acting on the blades. This is the force responsible for the lift. In the other hand, it is well known

the following transfer function between torque and input voltage:

$$\tau(s) = \frac{JK_t s + K_t B}{s^2 JL + (RJ + BL)s + RB + K_e K_t} u(s) \quad (25)$$

Where u is the voltage input, L is the inductance of the coil, K_e is the constant which links the induced voltage with the angular rate of the rotor; it depends on the permanent magnets and the coils on the motor. K_t is the constant which links the current owing through the coils of the motor to the generated mechanical torque.

To simplify the transfer function in equation 25, we could neglect the transient in the angular speed, ω. This would imply that the blades have no inertia, or $J = 0$. By making this assumption we obtain a new, simplified transfer function between τ and u:

$$\tau(s) = \frac{\frac{K_t}{L}}{s + \frac{R}{L} + \frac{K_e K_t}{BL}} u(s) \quad (26)$$

Comparing to equation 25, we see that we have lost the zero, which would describe the peak in torque necessary to accelerate the blades. We have also lost a possible oscillatory variation in torque, which could have occurred because of energy shifting from the magnetic field of the coil to the kinetic energy of the blades and vice versa. Even so, the approximation seems reasonable, provided the transient of ω will have little effect compared to the lasting torque generated by the friction of the blades with the air.

Given the above assumption that $J = 0$, we can write the torque equation for each rotor of the helicopter:

$$\tau_{top} = B\omega_{top} \quad (27)$$

$$\tau_{bot} = B\omega_{bot} \quad (28)$$

The two rotors spin opposite each other, and to keep the body from rotating, the two torques should cancel each other out $\tau_1 - \tau_2 = 0$. To make the body spin, but maintain the same lift, if the torque generated by one rotor increases, the other should decrease by the same amount. If Γ is the torque on the body of the helicopter and the two rotors change their torque with the same scalar amount (only in opposite sense), we can write:

$$\Gamma = \tau_{top} - \tau_{bot} = 2\Delta\tau \quad (29)$$

If we express $\Delta\tau$ according to the transfer function 26 we can write:

$$\Gamma(s) = \frac{2\frac{K_t}{L}}{s + \frac{R}{L} + \frac{K_e K_t}{BL}} \Delta u(s) \quad (30)$$

A PWM (Pulse-Width Modulation) signal in voltage controls the motors on the helicopter, and we now have a transfer function between Γ and u. However, the signal sent to the helicopter by the remote control does not control the torque on the body of the helicopter, but its angular rate. This makes sense, since it would be cumbersome to control an angle by the angular acceleration. If we consider r to be the angular rate of the body of the helicopter, J_h the moment of inertia of the body and B_h to be the friction coefficient of the body with air we can write the torque equilibrium:

$$\Gamma = J_h \frac{dr}{dt} + B_h r \quad (31)$$

Considering r is fairly small, we can neglect the air friction of the body and obtain:

$$\Gamma = J_h \frac{dr}{dt} \quad (32)$$

If we apply Laplace transformation, we obtain:

$$r(s) = \Gamma(s)\frac{1}{J_h s} \quad (33)$$

Substituting $\Gamma(s)$ according to equation 30we obtain:

$$r(s) = \frac{2\frac{K_t}{L}}{s + \frac{R}{L} + \frac{K_e K_t}{BL}} \frac{1}{J_h s} \Delta u(s) \quad (34)$$

The manufacturers of the helicopter use a gyroscope to measure r and a closed-loop for its control. A hypothetical model of what is implemented in the mixer circuit of the helicopter is presented in Figure-8. What we intend to identify is the system between the input and output boxes in this figure. If we close the loop for the transfer function from equation (34) and add a gain K for a proportional regulator, we will obtain:

$$\frac{\frac{2K_t}{LJ_h}}{s^2 + (\frac{R}{L} + \frac{K_e K_t}{BL})s + \frac{2KK_t}{LJ_h}} \quad (35)$$

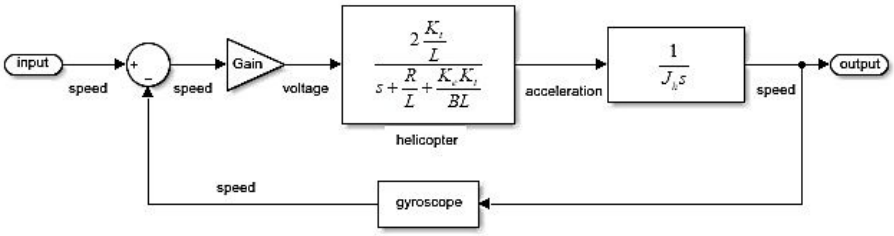

Figure-8. Hypothetical model of yaw control design.

3.2 Identification Using CIFER

The performance of frequency response methods can be enhanced by using powerful tools like CIFER. CIFER was developed by the Aero-flow dynamics Directorate (AFDD at Ames Research Center) in the 1980s, specifically for rotorcraft applications. It represents an integrated facility for system identification based on the frequency-response approach. The identification method used by CIFER is schematically presented in Figure-9 [12].

It consists of six analysis programs and a database for storing the input data time signals and the frequency response results. For this project, the CIFER Student Edition was used. The utilities used so far are FRESPID for determining the frequency response of the yaw channel.

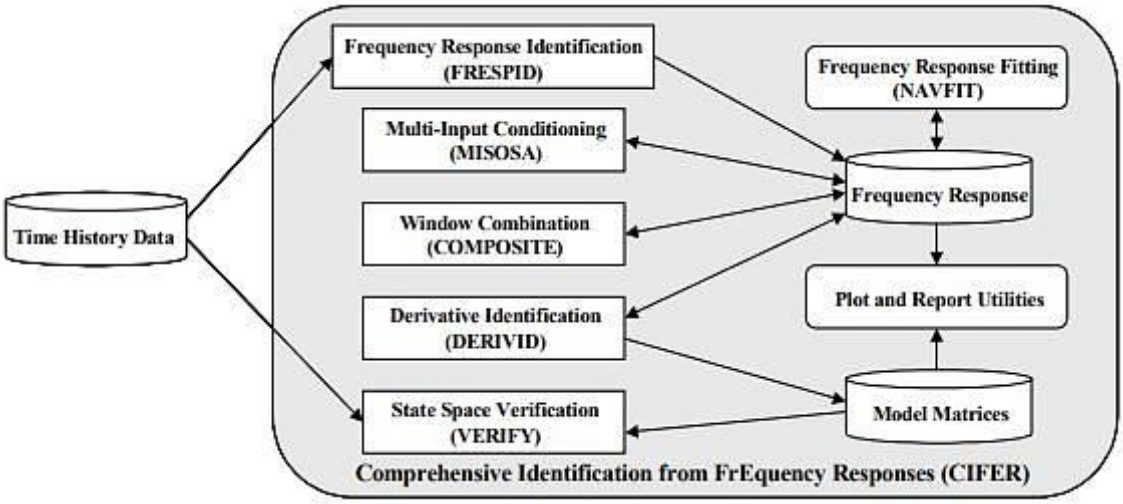

Figure-9. Frequency-domain system identification procedure (CIFER).

3.3 Identification using TFA

The control signal for the helicopter is PPM (Pulse Position Modulation), which is time-modulated. It takes around 12 ms to send a complete control frame. This is the most significant problem when applying the TFA method since it will be impossible to sample high-frequency sine waves accurately. This limited the identification experiments until frequencies of around 5 Hz. The lowest frequency chosen was 1Hz. The presented experiment was done for 20 seconds (sufficiently long to have a smooth passing between frequencies). The number of data points to each sample period was calculated from:

$$f_0 = 1Hz$$
$$f_1 = 5Hz$$
$$T = 20s$$
$$T_s = 0.012s$$

$$N_s = \frac{\frac{1}{f_1}}{T_s} = \frac{0.2s}{0.012s} = 16.6samples$$

At the beginning of the identification chirp signal, a pure sine was added, with the frequency of the first frequency in the chirp signal, to avoid the transient effects in the chirp signal. The signal was then filtered to remove the high-frequency noise produced by the rotors. A 10^{th} order low-pass Butterworth filter was used, with a cut-off frequency of 6 Hz. Due to its rotating masses, a helicopter is usually subject to intense vibration. If a rotor is slightly unbalanced or a rotor shaft is a bit tilted, vibrations will appear. The UAV helicopter makes no exception to this rule. Figure-10 shows the used signals for the experiments in the time domain.

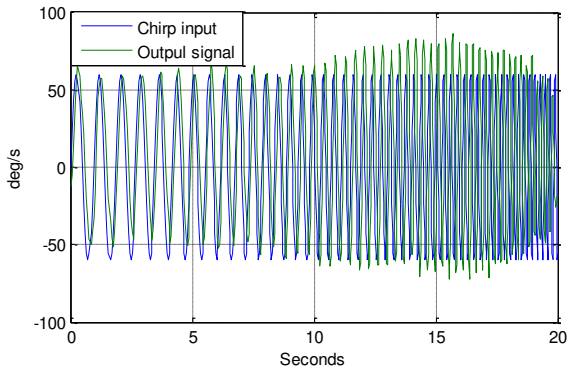

Figure-10. Input chirp signal and output system response.

The amplitude of the chirp signal varies from -0.2 to +0.2 (-60°/s and +60°/s). These values represent the percent of the total range of the stick position, which has a total variation between -1 and 1, corresponding to an angular velocity of approximatively-300°/s and +300°/s, respectively.

The frequency responses obtained using the TFA (green line) and CIFER (blue line) methods can be seen in Figure-11. The two results are quite close for the two methods, so a long time for the experiment is not needed.

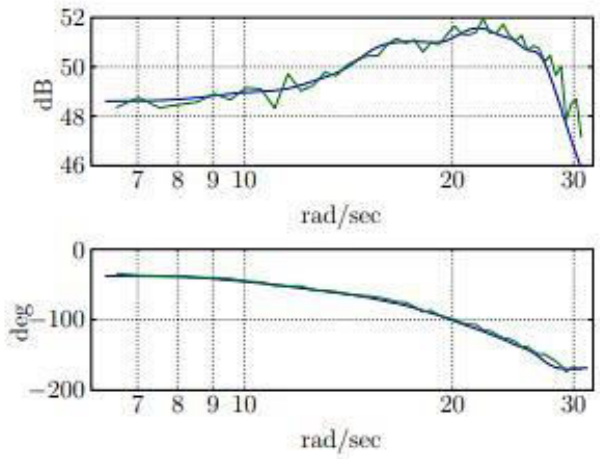

Figure-11. Bode rresponse obtained with TFA and CIFER.

A resonance peak around 22 rad/sec corresponds to a frequency of around 3.5 Hz. After this frequency, the magnitude decreases. Because of the sampling time limitations, we cannot see what happens with the system at frequencies higher than 8 Hz, but we can assume that the system's magnitude will continue to decrease.

The phase is continuously decreasing because of the dead time, mainly generated by the transmission delay. We can also conclude that the TFA method performs well.

4. CONCLUSIONS

The identification of the yaw movement of the helicopter was presented. The TFA identification was compared with an identification method using CIFER, a commercially available tool designed for aircraft identification. The two results are quite close for the two experiments. The phase was continually decreasing because of the dead time, mainly generated by the transmission delay.

A frequency-domain identification based on the TFA technique was developed and tested. The novelty of the study was to use variable sample time in the chirp signal used as the input for the identification. The purpose of this variable sample time was to have the same number of samples per cycle for all ranges of frequencies of the chirp signal. Thus the sampling period was varying according to the frequency to maintain the same sampling resolution for all frequencies.

The theoretical framework regarding the frequency response analysis was presented and followed by the practical implementation was widely explained. The TFA concept was used, considering as input just one identification signal called a chirp signal.

Parameters designs to have an appropriate chirp signal were considered. Suitable design parameters guarantee the generation of a useful signal for the identification purpose and can lead to considerable advantages in the cost-benefit relation during the real tests.

ACKNOWLEDGEMENT

The authors thank Ghent University Department of Electrical Energy Systems and Automation. The views expressed in this paper are not necessarily endorsed by the university mentioned above.

REFERENCES

[1] Ljung L. 1993. Some results on identifying linear systems using frequency domain data. In: Proceedings of 32nd Conference on Decision and Control; San Antonio, TX. pp. 3534-3538.

[2] Schoukens J. and Pintelon R. 1991. Identification of linear systems: a practical guideline to accurate modelling. London: Pergamon Press.

[3] Kollar I. 1994. Frequency domain system identification toolbox for use with Matlab. The Mathworks.

[4] De Vries D.K., Van den Hof P.M.J. 1998. Frequency domain identification with generalized orthonormal basis functions. IEEE Trans Autom Control. 43(5): 656-69.

[5] Pintelon R., Guillaume P., Rolain Y., Schoukens J., and Vanhamme H. 1994. Parametric identification of transfer functions in the frequency domain - A survey, IEEE Trans. Automation Control. 39: 2245-2260.

[6] Whitfield A.H. 1987. Asymptotic behavior of transfer function synthesis methods, Int. J. Control. 45: 1083-1092.

[7] Sidman M.D., De Angelis F.E. and Verghese G.C. 1991. Parametric system identification on logarithmic frequency response data, IEEE Trans. Automation Control. 36: 1065-1070.

[8] McKelvey T. and Akcay H. 1994. An efficient frequency domain state-space identification algorithm: Robustness and stochastic analysis, in Proc.33rd IEEE Conf. Decision Control, Lake Buena Vista, FL. pp. 3348-3353.

[9] Schoukens J. and Pintelon R. 1991. Identification of Linear Systems. A Practical Guideline to Accurate Modeling, Oxford, UK: Pergamon.

[10] Sendoya-Losada D.F., Quintero-Polanco J.D. 2018. PID controller applied to an Unmanned Aerial Vehicle, ARPN Journal of Engineering and Applied Sciences. 13(1): 325-334.

[11] Deac R., Neamtu D. 2009. Identification and computer control of a UAV helicopter, Master Thesis, Ghent University.

[12] M. B. Tischler. 2016. CIFER User's Guide Student Version 5.2.00. US Army ATCOM, Ames Research Center, Moffett Field, California, USA.